

# Time-series analysis of near-IR variabilities on VVV M dwarf stars towards the Milky Way's bulge

Thiago Ferreira dos Santos<sup>1</sup> & Roberto Kalbusch Saito<sup>1</sup>

<sup>1</sup>Departamento de Física, Universidade Federal de Santa Catarina, Brazil  
Contact: t.ferreira@astro.ufsc.br



## Near-Infrared Selection of M Dwarf stars

We emphasise our project on red dwarf stars of spectral type M using the VVV Survey (Minniti et al. 2010) multi-colour data-set of the Galactic bulge field VVV-b294, centred at  $(l, b) = (3.88^\circ, -3.14^\circ)$ . The main choice of such objects is based on the fact that their maximum emission occurs in near-IR wavelengths, the observation range of the VVV Survey and given the large fraction of those present in the Galaxy, red dwarf stars become one of the main targets to the search of potentially habitable, water-supported rocky exoplanets.

Giant and M dwarf stars present similar near-IR colours range, for example in  $(J - H)$  and  $(H - K_s)$  colours, which makes a photometric selection solely inefficient. We adopted a reduction proper motion  $H_J$  criteria (Rojas-Ayala et al. 2014) to perform a distinction between those two classes making use of astrometric data from Gaia EDR3 (Gaia Collab. et al. 2018), calculating  $H_J$  of selected objects according to eq. (1), adopting for M dwarf stars  $H_J > 68.9 \cdot (J - K_s) - 50.7$ . Moreover, we selected only stars with parallax  $\pi > 1 \text{ mas}$ , especially due to the proximity of M dwarf stars in the magnitude range of the VVV survey, then presenting higher proper motions, in contrast to red giant stars, further away however reddish due to extinction effects in the Milky Way.

$$H_J = J + 5 \log_{10}(\mu) = J + 5 \log_{10} \left( \sqrt{\mu_{\alpha \cos \delta}^2 + \mu_\delta^2} \right) \quad (1)$$

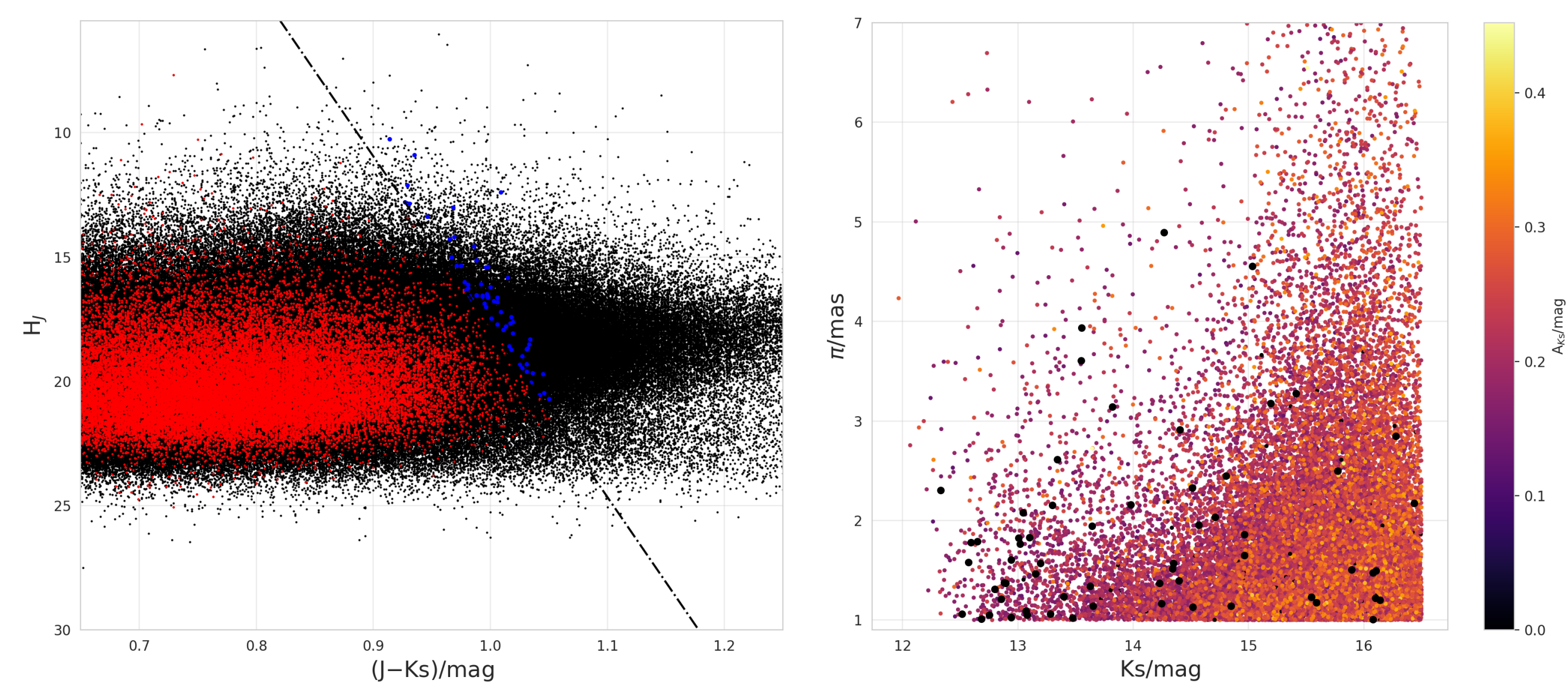


Figure 1. Left:  $(J - K_s)$  and  $H_J$  relationship for stars with  $K_s < 16.5^m$ . Right: Parallax  $\pi$  and  $K_s$  relationship for selected stars. The colour-index represents extinction levels in the line of sight of such stars in  $K_s$  filter. Blue (left) and black (right) dots indicate spurious red giant stars.

Photometric fluctuations on exoplanet-M dwarf systems lasts typically around  $0.15^m$  in  $K_s$  filter, therefore, we arbitrarily limited our selection in the VVV  $K_s^m$  PSF light-curves to  $K_s < 16.5^m$ , consequently reaching  $\sigma_{K_s} < 0.05^m$ , which is expected to reduce the incidence of false-positives in our analysis. Furthermore, based on their near-IR colours, we estimated the spectral subtype for M dwarf class as function of  $\xi := (Y - J)$ ,  $\eta := (Y - K_s)$  and  $\zeta := (H - K_s)$  colours, following eq. (2), also estimating the distance of such objects using the observational and theoretical magnitudes in  $J$ -filter (Rojas-Ayala et al. 2014).

$$M(\xi, \eta, \zeta) \triangleq 5.394(\xi) + 4.370(\xi)^2 + 24.325(\eta) - 7.614(\eta)^2 + 7.063(\zeta) - 20.779. \quad (2)$$

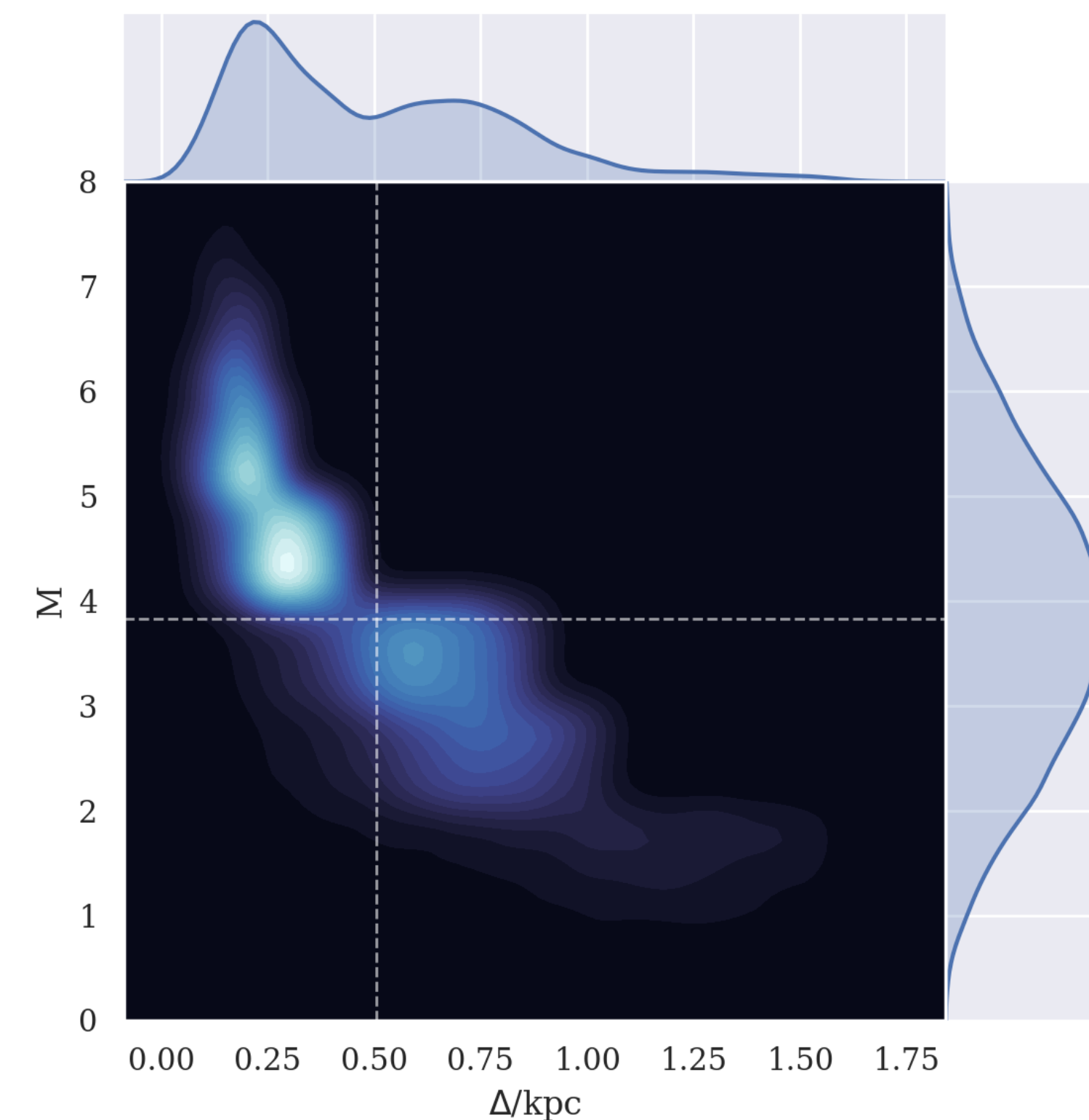


Figure 2. Density diagram for the spectral subtype for M dwarf stars and their distance. Dotted lines represent average values for such parameters as well as their distributions are presented on the sides.

The main objective of exoplanetary studies focuses on the detection of potentially habitable exoplanets, those orbiting a region around a star that primitively provides an adequate temperature for the existence of liquid-state water on its surface and the existence of  $\text{CO}_2/\text{H}_2\text{O}/\text{N}_2$  molecules and biomarkers as  $\text{O}_2/\text{O}_3/\text{CH}_4$  in their atmospheres (Kasting et al. 1993). However, silicates and pyroxenes unknown naturally in any terrestrial rock, e.g., Krinovite, Barringerite and Heideite may indicate numerous different chemical compositions both in the formation period and currently in those known extraterrestrial bodies, which may make environments unfeasible conducive to the presence and maintenance of organic life (Gaidos & Selsis 2007).

## Period finding algorithms

We chose, based on the orbital periods of rocky exoplanets orbiting in the habitable zone of M dwarf stars, minimum, maximum and spacing frequencies of  $f_{min} = 0.01 \text{ d}^{-1}$ ,  $f_{max} = 80 \text{ d}^{-1}$  and  $\delta f = (\beta \times W)^{-1}$ , where  $W$  corresponds the total time-span of the observations and  $\beta = 5$ , a counting periodogram factor. In opposition to commonly implemented Fourier-like sinusoidal methods or those based on Phase-folding methods, the Box-fitting Least Squares method (BLS; Kovacs et al. 2002) is a statistical method implemented to detect transit-like candidates by potential exoplanets (even exoplanetary systems or exomoons) modelling a periodic upside down box-like on a phase diagram. In cases where we have a non-uniform temporal distribution, the Lomb-Scargle (LS; VanderPlas & Ivezić 2015) method provides a straightforward solution based on a Fourier-like power spectrum to detect and fit a sine-like periodic component at an unevenly-sampled data-set. Similarly to the LS method, the Phase Dispersion Minimisation method (PDM; Stellingwerf 1978) is widely used to detect periodic components in data with a relatively large time difference between two subsequent observations, data that do not present a priori sinusoidal behaviour and data with a few observational epochs, which are often impediments to the use of methods based on Fourier transforms.

## Primary results

From the 1.906.710 sources presented in the VVV-b294 tile catalogue, 28.529 M dwarf stars were selected after the photometric and astrometric processes previously described, with 17.043 of them effectively analysed. We further selected those stars with equal periods on all the three before-mentioned methods, also excluding those stars with likely seasonal periods as exhibited in Fig. 4 (Ferreira et al. 2021). About 50 stars present high significance periods, which may be an indicator of exoplanetary transits. For those selected, we are also exploring the possibility to obtain radial velocity curves and spectra to validate and determine accurate parameters of the candidates.

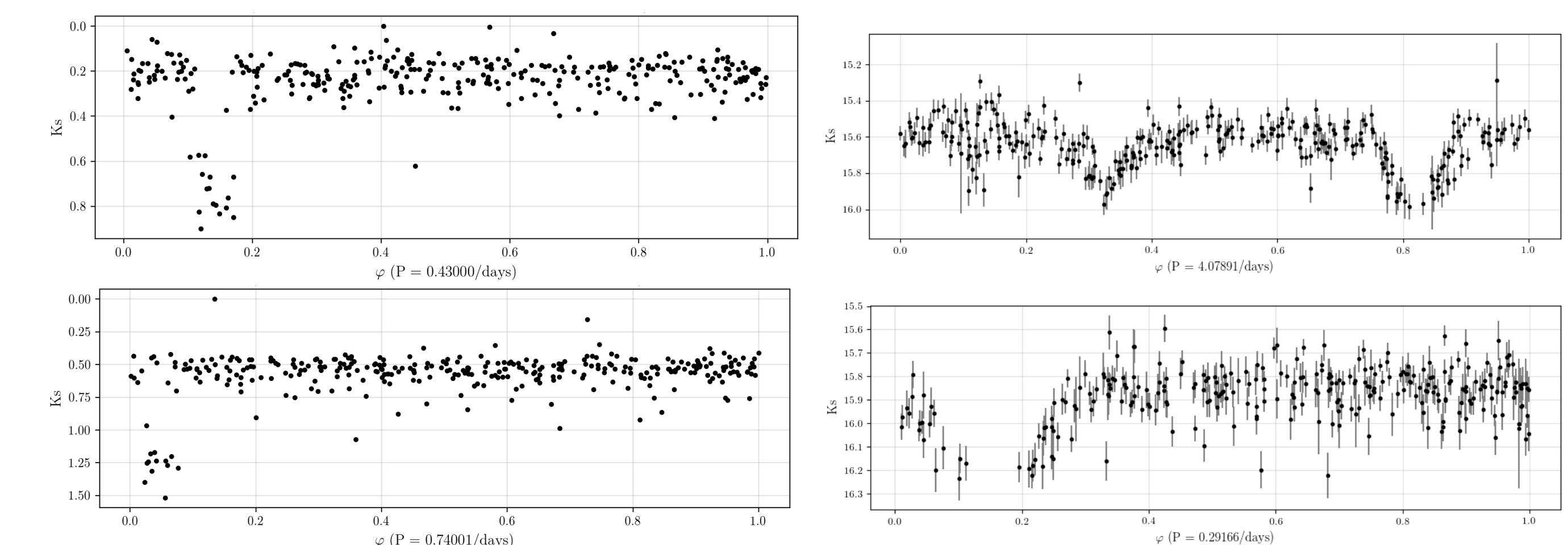


Figure 3. Simulated (left) and resulting (right) phase diagrams of selected objects.

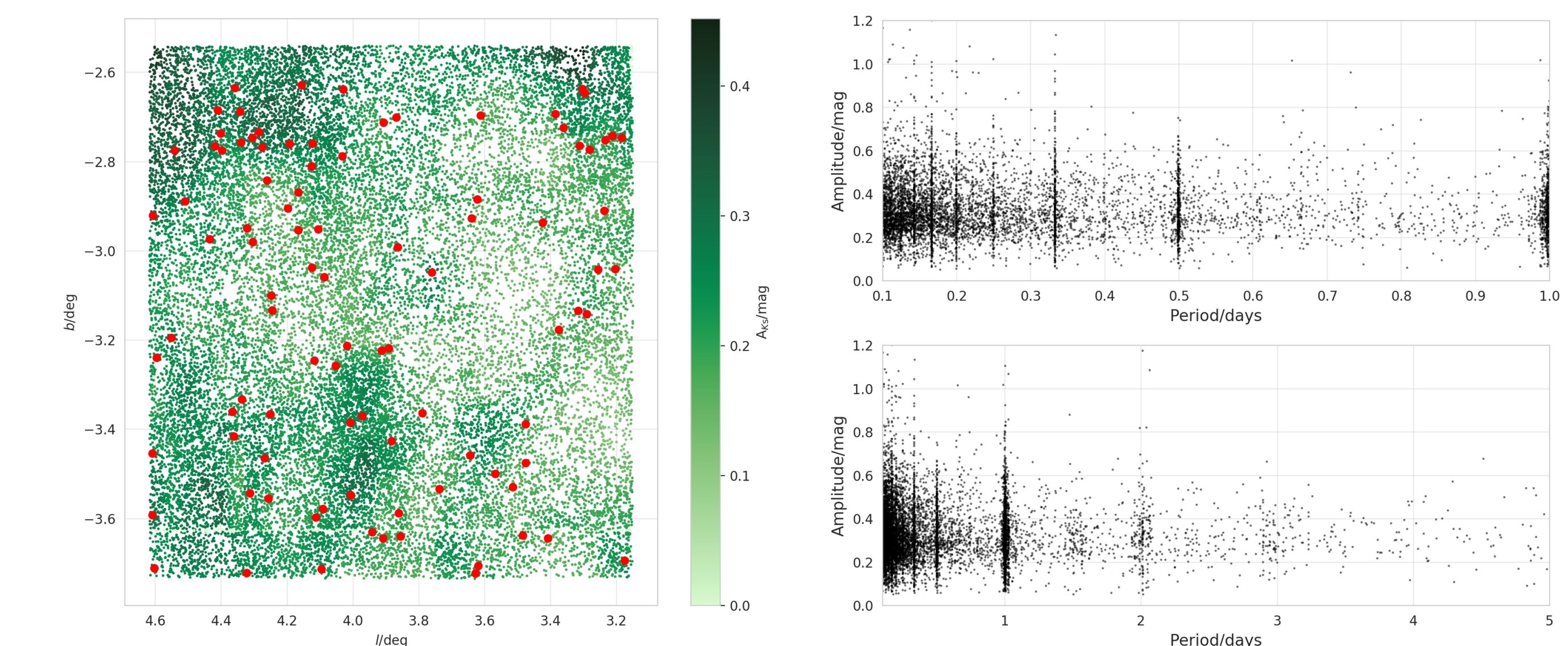


Figure 4. Left: Surface density distribution of the VVV M dwarf stars on tile b294, with red dots representing the 50 selected exoplanetary transit candidates. The colour index represents the extinction around  $1''$  of the star. Right: Relationship between the orbital periods and signal amplitudes for analysed stars. We note the presence of seasonal periods (fractions and multiples of 1 day), which were removed considering the interval  $P \pm 0.01$  days. Those one day periods may arise from the period corresponding to diurnal aliasing, which may induce false periods.

## Bibliography

- |  |   |
|--|---|
| Ferreira et al. 2021, in prep.   | Minniti, D., et al., 2010, <i>NewA</i> , 15, 433-443.     |
| Gaia Collaboration, et al., 2021, <i>A&amp;A</i> , 649A, A1.           | Rojas-Ayala, B., et al., 2014, <i>A&amp;A</i> , 571, A36. |
| Gaidos, E. & Selsis, F., 2007, <i>Protostars and Planets V</i> , P929. | Stellingwerf 1978, <i>ApJ</i> , 224, 953                  |
| Kasting et al., 1993, <i>Icarus</i> , 101, 108                         | VanderPlas & Ivezić 2015, <i>ApJ</i> , 812, 18V           |
| Kovács, G., et al., 2002, <i>AA</i> , 391, 369.                        |   |

We gratefully acknowledge the use of data from the ESO Public Survey programme ID 179.B-2002 taken with the VISTA telescope and data products from the CASU. T. F. acknowledge support from PIBIC@UFSC and CNPq-Brasil.